

CHAPTER 3

DOXYCYCLIN-INDUCIBLE EXPRESSION OF SPARC/ OSTONECTIN/ BM40 IN MDA-MB-231 HUMAN BREAST CANCER CELLS RESULTS IN GROWTH INHIBITION

Summary

SPARC (secreted protein acidic and rich in cysteine) / BM40/ osteonectin is a matricellular protein with multiple effects on cell behaviour. *In vitro*, its major known functions are anti-adhesion and anti-proliferation, and it is associated with tissue remodelling and cancer *in vivo*. SPARC is overexpressed in many cancers, including breast cancer, and the effects of SPARC seem to be cell type specific. To study the effects of SPARC on breast cancer, we transfected SPARC into the MDA-MB-231 human breast cancer cell line using the Tet-On inducible system. By Western analysis, we found low background levels in the MDA-MB-231 and clone X parental cells, and prominent induction of SPARC protein expression after doxycyclin treatment in SPARC transfected clones X5, X21, X24 and X75. Induction of SPARC expression did not affect cell morphology or adhesiveness to collagen type I and IV, but it slowed the rate of proliferation in adherent cultures. Cell cycle analysis showed that SPARC slowed the progression to S phase. Doxycyclin induction of SPARC also slowed the rate of closure in the culture wound healing assay. Thymidine inhibition of proliferation abrogated this effect, confirming that it was due to anti-proliferation rather than inhibition of migration. Consistent with this, we were unable to detect any differences in migration and Matrigel outgrowth analysis of doxycyclin-stimulated cells. We conclude that SPARC is inhibitory to human breast cancer in contrast to its

stimulatory effects reported for melanoma and glioma cells. Similar growth repression by SPARC has been reported for ovarian cancer cells, and this may be a common feature among carcinomas.

Introduction

SPARC (secreted protein acidic and rich in cysteine) is a 32 kDa glycoprotein that is secreted by many different types of cells, but principally those of mesenchymal origin. It is also known as BM40 [2], since it is a component of basement membrane matrix, and as osteonectin, since it has affinity for bone matrices [3]. SPARC is a matricellular protein; It bridges the gap between cells and the extracellular matrix (ECM) to mediate cell-matrix interaction, but does not serve a primary structural role [38]. SPARC expression in the adult is largely limited to tissues undergoing repair or remodeling such as bone growth and wound healing, and elevated expression of SPARC is found in many pathologies [53].

In vitro, the two major effects of SPARC on mesenchymal cells are anti-adhesion and anti-proliferation. Exogenous SPARC added to cells in culture has been shown to induce a round morphology in confluent monolayers of bovine smooth muscle cells, fibroblasts and endothelial cells, and to maintain the rounded morphology of newly plated fibroblasts by inhibiting their spreading [49]. Exogenous SPARC inhibited the incorporation of [3H]-thymidine by as much as 90% in synchronized cultures of bovine aortic endothelial cells [74]. However, the effect of SPARC on proliferation is cell type-specific. It does not affect the growth of melanoma [35] or prostate cancer cell lines [73], but reduces the growth of ovarian cancer cell lines [75]. SPARC is downregulated upon transformation of fibroblasts [10] [87], and upregulated during late differentiation of keratinocytes [200] and

skeletal myoblasts [201]. It is prominently expressed by the retinal pigment epithelium of the eye and lack of SPARC leads to cataracts in SPARC null mice [66]. Moreover, mesangial cells, fibroblast and aortic smooth muscle cells derived from SPARC null mice proliferate faster than wild-type counterparts [76]. SPARC can also effect cell migration. It is haptotactic for renal cell carcinoma cells in Boyden chamber assays [86], and promotes prostate and breast cancer cell chemotactic migration and invasion *in vitro* [73]. These data suggest a role for SPARC in mediating metastasis to bone by these different carcinoma types.

We previously found that SPARC was selectively expressed by a series of invasive breast cancer cell lines studied [36]. These cell lines can be distinguished from their non-invasive counterparts by a comparative loss of epithelial attributes in preference for mesenchymal features [202]. This is consistent with the preferential expression of SPARC by mesenchymal cells rather than epithelial cells, although, as mentioned above, this is not exclusive. Breast cancer cells that have undergone an epithelial to mesenchymal transition may show heightened responsivity to SPARC. Indeed, all invasive human breast cancer cell lines responded to SPARC with increased activation of matrix metalloproteinase-2 (MMP-2)/ gelatinase A, an extracellular protease capable of degrading basement membrane specific, type IV collagen [36]. To study further the effect of SPARC on human breast cancer cells, we engineered the MDA-MB-231 cell line, which expresses very low levels of SPARC, with a DOX-inducible vector to control SPARC expression, and examined the biochemical and biological consequences. Unlike melanoma and glioma cells that respond to SPARC with increased migration and invasion, the MDA-MB-231 cells showed reduced proliferation.

Experimental procedures

Cell culture and reagents

MDA-MB-231 human breast cancer cells, originally obtained from the ATCC (Rockville, MD, USA), were cultivated in DMEM (Life Technologies, Grand Island, NY, USA) supplemented with 10% fetal calf serum (DMEM-FCS) (CSL Limited Biosciences, Parkville, Victoria, Australia). Bovine aortic endothelial (BAE) cells were used at passage 8 and also cultivated in DMEM-FCS. Cultures were maintained at 37 °C in 5% CO₂. Doxycyclin hydrochloride (DOX; Sigma, St. Louis, USA) was used at 2 µg/ml unless otherwise specified. Matrigel was kindly provided by Dr. Hynda Kleinman, NIDCR, NIH, USA. SPARC purified from bovine bone was purchased from Haematologic Technologies Inc, VT, USA, and recombinant human SPARC purified from transfected HEK293 cells [72] was kindly provided by Prof. Rupert Timpl, Max-Plank-Institut Für Biochemie, Germany.

Plasmids

The pUHG17-1, pUHC13-3 and pUHD10-3 were kindly provided by Prof. H. Bujard, Department of Molecular Biology, University of Heidelberg, Germany [203, 204]. The pUHG17-1 plasmid contains the rtTA transactivator gene. The pUHD 10-3 plasmid contains seven repeats of the tet operator linked to a cytomegalovirus minimal promoter, upstream from the multiple cloning site and a simian virus 40 polyadenylation signal. The SPARC cDNA, hon-2 [9] (kindly provided by Dr. Larry Fisher, NIH) was partially digested with EcoRI and subcloned into pUHD10-3 to generate pUHD10-3-SPARC. pUHC13-3 contains the luciferase cDNA under an rtTA responsive promoter. The pSV40Zeo plasmid encoding Zeocin resistance (Promega, Madison, WI, USA) and pCHC6 [205] encoding hygromycin resistance

were used as selective markers for the first and second rounds of transfection, respectively. All plasmids were prepared by QIAGEN mini and maxi plasmid preparation kits (QIAGEN Pty Ltd, Victoria, Australia).

Transfection

To generate SPARC-inducible clones, we performed 2 rounds of transfection. In each case, the MDA-MB-231 were plated overnight (200,000 cells per well) in 6-well-plates in DMEM-FCS. For the first round transfection, 2 μg of pUHG17-1 and 0.2 μg of pSV40Zeo were cotransfected the next day using Fugene (4 μl ; Boehringer Mannheim, USA). Clones were selected in the presence of 800 $\mu\text{g}/\text{ml}$ of Zeocin (Invitrogen, The Netherlands) and cloned using cloning cylinders. RNA from each clone was extracted and expression of rtTA was assessed by RT-PCR. High expression clones were further assessed by transient transfection with pUHC13-3 in the presence of 2 $\mu\text{g}/\text{ml}$ of DOX for 48 hours. Cell lysates were collected for analysis with the Luciferase assay system (Promega) as per manufacturers guidelines. We also performed transient transfection with pUHD10-3-SPARC in the presence of 2 $\mu\text{g}/\text{ml}$ DOX, and conditioned media were analysed for SPARC by Western blot. Collectively these assays identified 3 clones (X, Y and Z) with the highest expression of rtTA in the presence of DOX, and lowest in its absence.

For the second round transfection, each of the 3 clones (X, Y and Z) were cotransfected with 2 $\mu\text{g}/\text{ml}$ of pUHD10-3-SPARC and 0.2 μg of pCHC6 using Fugene (4 μl). The clones were selected in the presence of 600 $\mu\text{g}/\text{ml}$ Hygromycin B (Gibco BRL, Scotland). To rapidly screen for strong expression, clones were initially grown in the presence of 2 $\mu\text{g}/\text{ml}$ DOX for 72 hours and the conditioned media were collected and subjected to Western analysis for SPARC. Those with high expression

were further tested in the presence and absence of DOX to identify clones with the lowest baseline and highest inducibility. Those clones (X5, X21, X24 and X75) were selected for further work. High background was found in clones derived from Y, and only low levels of SPARC were achievable in clones derived from Z, so these were not used further.

Western analysis

Analyses of SPARC expression in the MDA-MB-231 and transfected clones were performed on conditioned media (1 ml in a 6-well plate). Proteins in the unconcentrated conditioned media from clones were separated under reducing conditions using 10% SDS-PAGE. Loading was standardized for equal amount of total protein from each cell lysate. The proteins were then transferred to PVDF membrane (Immobilon, Millipore Corp., Bedford, MA, USA) for immunoblotting. Transfer was monitored by reversible staining with Ponceau Red (Sigma). The blots were blocked for 2 hours with blocking solution (5% skim milk, 0.05% Tween 20 in PBS pH 7.5) and then incubated with primary antibody (Anti-Osteonectin, Haematologic Technologies Inc., 5.4 µg/ml) in blocking solution overnight at 4°C. The membrane was then washed 3 times for 10 minutes with blocking solution and incubated for 1.5 hour at room temperature with horseradish peroxidase (HRP)-conjugated goat anti-mouse IgG antibody (Pierce, IL, USA) diluted 1:20,000. Signals were developed with an enhanced chemiluminescence (ECL) kit according to the manufacturer's instructions (Pierce).

Adhesion assay

Collagen type I (Vitrogen100, Cohesion, CA, USA) and IV (Sigma) dilutions (2.5, 1, 0.5, 0.25, 0.125, 0.05 $\mu\text{g/ml}$) were prepared in DMEM with 0.1% BSA (DMEM-BSA) and added (50 μl per well) in triplicate to 96-well plates, and incubated for 60 minutes at 37°C. Wells were then washed with 100 μl of PBS containing 3% (w/v) BSA for 30 minutes at 37 °C. Cells were harvested from routine culture with PBS containing 0.2 mg/ml EDTA, washed twice in DMEM-BSA, and resuspended at 2.5×10^5 cells/ml DMEM-BSA. The cells were incubated with occasional mixing for 60 minutes at 37°C to allow for recovery of cell surface receptors. Cells (2.5×10^4 in 100 μl of media) were added to each well and incubated for 60 minutes at 37°C. The supernatant was removed from each well and the attached cells stained by the addition of 100 μl of Crystal Violet (0.5 % (w/v) in 25% (v/v) methanol) for 5 minutes at room temperature. Wells were gently rinsed 5 times with water to remove unbound stain and allowed to air-dry at room temperature. Even distribution of cells indicated even coating of the wells with each substrate. Bound crystal violet was solubilized with 100 μl /well of 0.1 M sodium citrate containing 50% (v/v) ethanol for 10-15 minutes at room temperature, and absorbance read at 540 nm (Power Wave X, Bio-Tek Instruments, Inc., Winooski, VT, USA).

Proliferation assay

Cells (1,000 cells per well) were plated in 96-well plates in DMEM-FCS (200 μl per well). Each clone was grown in the presence or absence of 2 $\mu\text{g/ml}$ of DOX (5 wells/treatment). One plate was fixed each day for the next 10 days, with 50 μl per well of cold 50% (w/v) trichloroacetic acid (TCA, Sigma) for 1 hour at 4°C. The supernatant was then discarded, and plates were washed 5 times with distilled water

and air-dried. After 10 days, all 10 plates were stained with sulforhodamine B solution (SRB, 0.4% w/v in 1% acetic acid; 100 μ l per well) (Sigma), and incubated for 10 minutes at room temperature. Unbound SRB was removed by washing 5 times with 1% acetic acid, the plates were air-dried, and bound stain was solubilized with 10 mM Tris-buffered saline and the optical densities read at 515 nm. Statistical analysis was performed using the General Linear Model program in SPSS (Chicago, Illinois, USA) and Linear Regression Analysis in GraphPad Prism 3 (GraphPad Software, San Diego, CA, USA).

Cell cycle analysis

Cells (2.5×10^5) were seeded in a 10 cm plate with or without 2 μ g/ml of DOX in DMEM-FCS. The medium was replaced 48 hrs later with fresh DMEM-FCS and the continued presence or absence of DOX. After an additional 24 hrs, the cells were trypsinized (0.025%, CSL Ltd., Victoria, Australia) washed with PBS-BSA and fixed in 1 ml of paraformaldehyde at 4°C for 10 minutes. Then the cells were collected by centrifugation (1500 rpm for 5 minutes), resuspended in 1 ml of 0.1% Triton X-100 and left at 4°C for 10 minutes. The cells were again centrifuged and resuspended in 1 ml of solution containing 50 μ g/ml propidium iodide (Sigma), 0.1% sodium citrate and 1 μ g/ml RNase. The stained cells were analyzed within 24 hr on a FACSCalibur instrument (Becton Dickinson, USA).

Wound healing assay

Cells (50,000 cells/well) were plated in 24-well plates in DMEM-FCS and grown to approximately 80% confluency. The monolayer was wounded by scraping a line across the well using a sterile 1 ml blue pipette tip, after which the culture was washed twice with DMEM and the media were changed to DMEM-BSA with or

without 2 $\mu\text{g/ml}$ of DOX and with or without 10 mM thymidine (Sigma). The monolayer wound was photographed everyday from day 0-4 at the same spot, guided by markings under the plate. The width of the wound was measured from each photograph and the closure expressed as % day 0. Statistical analysis was performed with the General Linear Model program in SPSS.

Chemomigration assay

Cell migration was determined using a 48-well microchemotaxis chamber assay (Neuroprobe, Cabin John, MD, USA) as described previously [206]. Cell migration was quantified by the number of cells that migrated directionally through a collagen I (10 $\mu\text{g/ml}$) coated 8 μm pore polyvinyl pyrrolidone-free polycarbonate filter (Poretics, Livermore, CA, USA) toward the chemoattractant. Briefly, cells (1×10^6 cells/ml), either pretreated or untreated with 2 $\mu\text{g/ml}$ of DOX for 48 hours, were resuspended in DMEM-BSA and loaded into the top chamber. Fibroblast conditioned medium was used as the chemoattractant and loaded into the bottom chamber. Chambers were incubated at 37°C in 5% CO₂ for 4 hours, after which the filters were removed, fixed and stained with Diff-Quik (Baxter Scientific, McGaw Park, IL, USA) and mounted on glass slides. Nonmigrated cells were removed by wiping with a cotton swab. At least four random fields of vision/well (x20 objective) were counted for quantitation of cell migration. Triplicate wells were performed in each assay.

Matrigel outgrowth and radial outgrowth

In vitro invasion analysis was performed with a novel adaptation of the Matrigel outgrowth assay [207]. Briefly, cells were trypsinized, counted, centrifuged

and resuspended in Matrigel to give densities of 250, 500 and 1000 cells per 5 μ l of Matrigel. Five microlitres of Matrigel containing cells was placed in each well (96-well ELISA plate) and let set in an incubator at 37°C in 5% CO₂ for 1 hour. After that, 80 μ l of DMEM-FCS with or without 2 μ g/ml of DOX was added on top of the droplet. For radial outgrowth, after the Matrigel droplet was set, 80 μ l of 2 μ g/ml collagen type I (Vitrogen100) was overlaid and incubated at 37°C in 5% CO₂ for 1 hour to set. This was followed by 80 μ l of DMEM-FCS with or without 2 μ g/ml of DOX. Cell morphology was observed and photographed daily.

Results

Detection and regulation of SPARC protein expression

To evaluate the level of SPARC protein expression in parental MDA-MB-231 cells, clone X parental and transfected clones X5, X21, X24 and X75, we performed Western analysis of serum free conditioned media generated in the presence or absence of 2 μ g/ml of DOX. Previously we found SPARC to be expressed in invasive breast cancer cell lines, BT-549 and Hs578T but not in MDA-MB-231 by Northern analysis [36]. Here, we found low levels of SPARC in MDA-MB-231 cultures after 4 days, and the level of expression did not change after DOX treatment (figure 3.1A). A similar level of expression was also found in clone X parental cells prior to SPARC transfection. After SPARC transfection, basal levels of expression in clones X5, X24 and X75 remained low but could be highly induced after DOX treatment. Clone X21 showed somewhat higher basal expression of SPARC in the absence of DOX, but this level could still be dramatically increased by DOX.

Addition of a range of DOX concentrations from 0.01-2 μ g/ml to clone X5 induced concentration-dependent expression of SPARC (figure 3.1B) and higher

concentrations up to 8 $\mu\text{g/ml}$ showed no increased expression (data not shown). Comparative Western analysis with commercial preparations of SPARC isolated from bovine bone at the stated concentration allowed estimation of the SPARC accumulation from clone X5 after 3 days of DOX-treatment to be around 5 $\mu\text{g/ml}$ (data not shown).

SPARC has no effect on morphology of transfected clones or on their attachment to collagen type I or IV

Despite pronounced effects on “rounding” of endothelial cells, smooth muscle cells and fibroblasts [49], we did not observe any changes in cell morphology after DOX treatment of our SPARC- transfected clones (data not shown). Similarly, addition of up to 100 $\mu\text{g/ml}$ exogenous, purified or recombinant SPARC did not alter MDA-MB-231 cell morphology, but did induce rounding of bovine aortic endothelial cells (data not shown). SPARC is known to have an anti-adhesive effect on certain cell types, achieved in part by the dissolution of focal adhesion complexes and reorganization of actin stress fibers [38]. Neither parental MDA-MB-231 cells, parental clone X or transfected clones showed any changes in cell attachment to collagen type I after pre-treatment with DOX for 3 days (figure 3.2). Concentration-dependent increases in attachment were seen from 0.05 $\mu\text{g/ml}$ up to 2.5 $\mu\text{g/ml}$ collagen type I for each clone, but there was no difference between the DOX-treated and untreated group (data not shown). Similarly, no difference was found between the two groups in adhesion to collagen type IV, a substrate to which the cells attach with a lower affinity (data not shown). We further tested the effects of SPARC-enriched (+DOX) or control (-DOX) conditioned medium on the subsequent attachment of these cells to either collagen type I or IV, but no difference was seen (data not

Collagen I concentration = 2.5 ug/ml

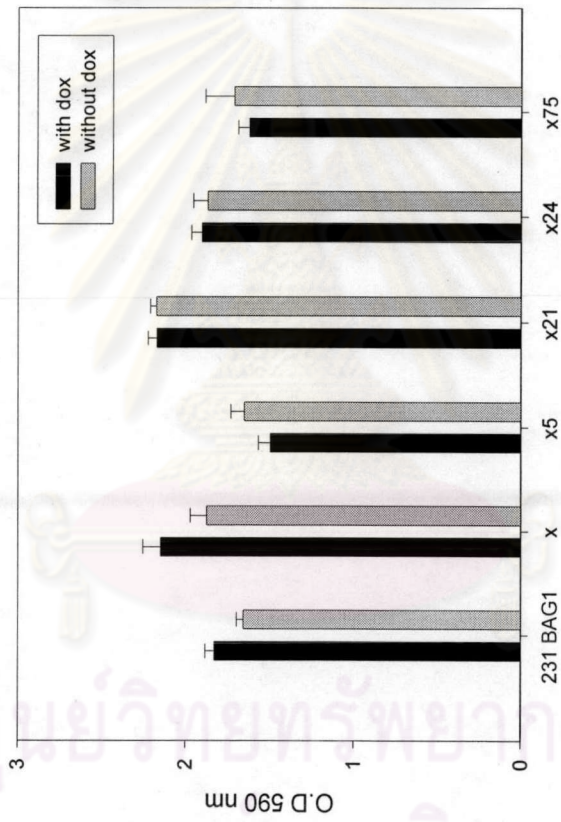


Figure 3.2: DOX-induced SPARC expression has no effect on cell attachment to collagen I coated plates. The MDA-MB-231 cells, clone X parental cells, and clones X5, X21, X24 and X75 were plated on collagen I coated plate in triplicate and analyzed for attachment after 1 hour as described in Material and Methods

shown). SPARC does not appear to affect the adhesion of these cells to collagen type I or IV.

SPARC inhibits anchorage-dependent proliferation in transfected clones

We then looked at the effect of DOX-induced SPARC on proliferation of the transfected MDA-MB-231 cells as numerous studies have reported differential effects of SPARC on cell proliferation. In the control MDA-MB-231 parental (not shown) and clone X parental cells (figure 3.3A), DOX had no effect on growth. The cells grew to confluency over the 10-day period in both DOX-treated and -untreated groups. However for each of the SPARC transfected clones, the DOX-treated group showed a slower rate of proliferation (shown in figure 3.3B for clone X24; clones X5, X21 and X75 data not shown). DOX treatment of all SPARC-transfected clones caused a delay in the time taken to reach half maximal growth (figure 3.3C), but each clone finally reached the same confluency. DOX was only added on the first day of the experiment so as to avoid media changes and allow the cultures to accumulate SPARC. A more pronounced inhibition may have been seen with repeated addition of DOX. However, this small but significant growth inhibition was reproducible and consistent between 5 replicates of each group in 3 independent experiments.

Cell cycle analysis

To analyse the growth effect further, we grew the MDA-MB-231 parental and clone X5 cells in the presence or absence of DOX, and harvested them for analysis of cell cycle distribution. As shown in figure 3.4, DOX at 2 $\mu\text{g/ml}$ did not influence the cell cycle distribution of the MDA-MB-231 parental cells. For clone X5, increasing concentrations of DOX from 0-2 $\mu\text{g/ml}$ showed a concentration-dependent reduction of the proportion of cells in S phase.

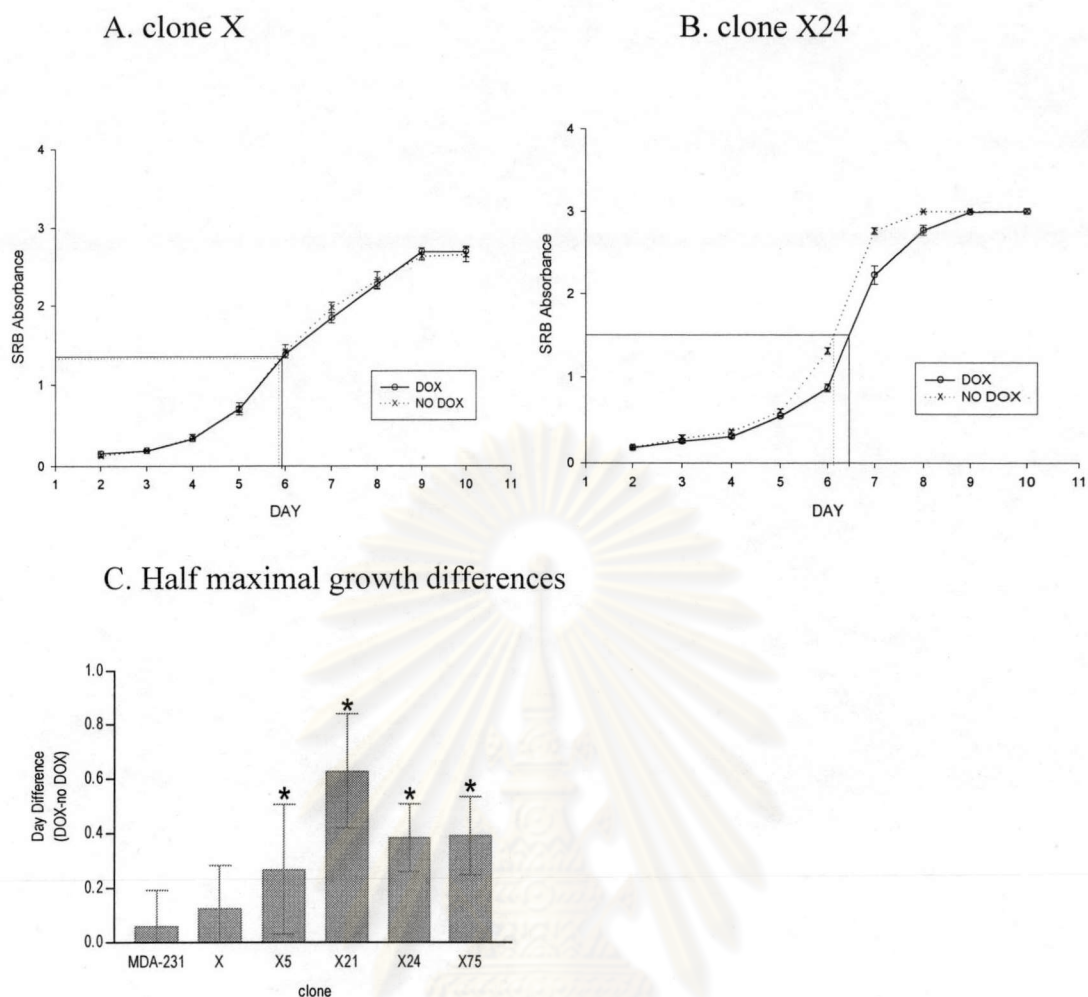
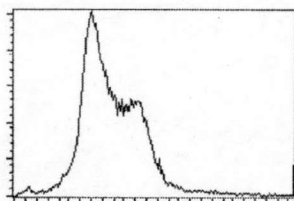
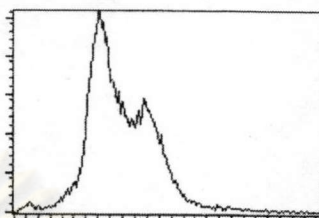


Figure 3.3: *In vitro* proliferation analysis of parental and transfected clones. Cells were seeded in 96-well plates in DMEM-10% FCS with or without 2 $\mu\text{g/ml}$ of DOX. Proliferation was measured everyday as described in Material and Methods. A, B Growth curves of clone X parental and clone X24 cells respectively. The solid line indicates the DOX-treated group and the dotted line indicates the untreated group. In B, statistical analysis showed a significant difference in growth kinetics ($P < 0.001$). C. The difference in time taken to reach half maximal growth in the presence compared to the absence of DOX. 95% confidence intervals are shown. * denotes significant difference ($P < 0.05$).

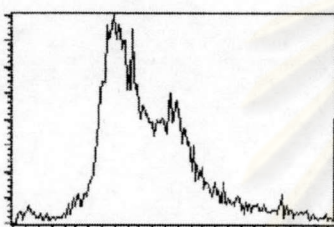
A. MDA-MB-231 control



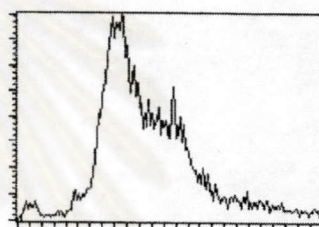
B. MDA-MB-231 + DOX 2 ug/ml



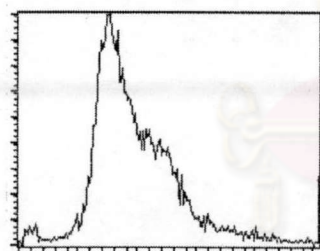
C. X5 control



D. X5 + DOX 0.02 ug/ml



E. X5 + DOX 0.2 ug/ml



F. X5 + DOX 2 ug/ml

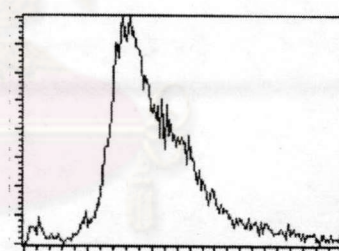


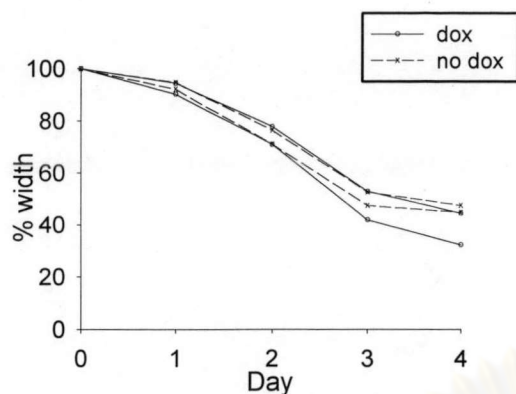
Figure 3.4: Cell cycle analysis of representative clones. The MDA-MB-231 (A, B) and clone X24 (C-F) were cultured in the presence or absence of DOX (0.02, 0.2 or 2 $\mu\text{g/ml}$) for 72 hours prior to cell cycle analysis by flow cytometry

DOX-induced SPARC slows down monolayer wound healing but has no effect on cell migration or Matrigel outgrowth.

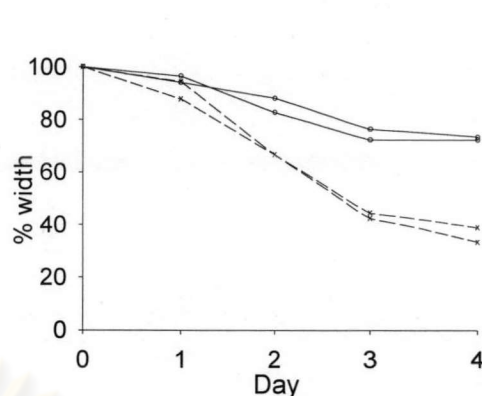
To assess the composite effects of the SPARC on cellular remodelling *in vitro*, we performed the cultured monolayer wound healing assay over 4 days. In this assay, closure of the wound depends on both proliferation and migration of the cells. Since SPARC is secreted and present in the conditioned media around the cells, it might work chemokinetically as reported in melanoma cells [35]. As shown in figure 3.5, however, clone X5 showed a slower rate of wound closure when SPARC expression was stimulated with DOX. Similar changes were seen in clones X21, X24 and X75 (data not shown) while clone X parental cells consistently showed no response to DOX. Also, there was no difference between the DOX-treated and -untreated MDA-MB-231 parental cells, which reproducibly showed a quicker rate of closure than the other clones (data not shown). To delineate the proliferative component, we performed this assay in the presence of 10 mM thymidine, which blocks cell proliferation (figure 3.5C inset). As shown in figure 3.5C, we found no effect of DOX on the rate of closure in the presence of thymidine, and furthermore, the capacity for wound closure was returned to non-DOX levels. These data confirmed the anti-proliferative effect of SPARC, and suggest that there is no chemokinetic effect of SPARC in our system.

Consistent with this, we were unable to detect any difference in the 48-well microchemotaxis migration of DOX-treated versus -untreated clones towards fibroblast conditioned media over 4 hours on collagen type I coated filters, even when the conditioned media from each culture was added into the chamber (data not shown). Similarly, long-term culture in 3-dimensional gels of collagen or Matrigel did not show any differences (data not shown).

A. clone X



B. clone X5



C. clone X5 in the presence of 10 mM thymidine

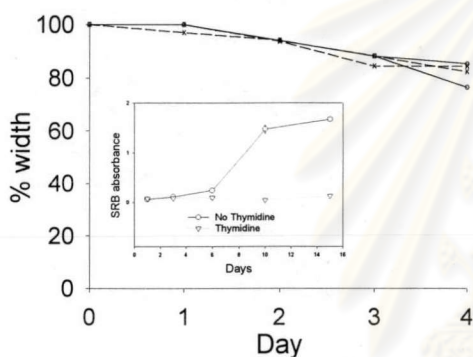


Figure 3.5: Cultured wound healing assay of clone X parental (A) and clone X5 (B) cells. Clone X5 cells were also tested in the presence of 10 mM thymidine (C). Inset in C shows the abrogation of MDA-MB-231 cell proliferation by 10 mM thymidine. Cells were plated and wounded in the presence or absence of 2 $\mu\text{g}/\text{ml}$ DOX. A photograph was taken each day for a period of 4 days and the width of the wound was measured. The starting size of each wound was designated as 100%. Data are presented from duplicate wells in one representative experiment of three independent experiments performed. In B, statistical analysis showed significant differences in wound closure between the DOX-treated and -untreated cells (P -value = 0.008).

Discussion

SPARC is a secreted protein found in remodeling tissues, and has dramatic effects on cell behaviour *in vitro*. First purified as a major non-collagenous component of bovine bone [3], its biological significance was linked to the regulation of bone mineralization. Later studies showed expression of SPARC also in non-mineralized tissue including gut, skin, liver, vascular smooth muscle cells and platelets [12, 19, 20, 25].

SPARC is overexpressed in many cancers. Malignancies of mesenchymal origin consistently exhibit strong immunostaining of SPARC [20]. It is overexpressed during neoplastic progression of human melanoma [28], meningioma [81], and glioma [82], and is associated with invasiveness. Many epithelial tumours exhibit high levels of SPARC [20], including esophageal carcinoma [30], hepatocellular carcinoma [29], prostate carcinoma [31] and breast carcinoma [32, 33]. Despite intensive immunostaining of SPARC in the carcinoma parenchyma, *in situ* hybridisation studies show that SPARC is usually produced by the surrounding stromal cells. This appears to be the case for breast [32] and hepatocellular [29] carcinoma, but both stromal and parenchymal cells were found positive in prostate carcinoma [31]. Ovarian carcinoma is rather unique, since the normal ovarian surface epithelium is positive for SPARC expression, and this is lost from ovarian carcinoma [75].

In vitro, SPARC is expressed in many cell lines including glioblastoma [34], melanoma [35], and prostate cancer cell lines [31]. For breast cancer cell lines, our previous work showed SPARC not to be expressed by better-differentiated lines like T47D and MCF-7, but expressed in cell lines that have acquired mesenchymal features such as BT-549, MDA-MB-435 and Hs578T [36]. In the present study, we further found that the mesenchymal-like MDA-MB-231 cells also expressed SPARC,

but at a lower level. This is consistent with its expression *in vivo* by carcinoma-associated fibroblasts and by tumour cells of mesenchymal origin. The low levels of SPARC produced by the MDA-MB-231 cells, and their continued co-expression of keratin as well as vimentin [208], may suggest that they will show behavioural tendencies of both epithelioid and mesenchymal cells, with respect to SPARC responsivity. Further analysis in a panel of breast cancer cell lines will be required to answer this question more fully. Approximately 10-15% of breast tumours show vimentin expression as a putative indicator of mesenchymal trans-differentiation [202], however, SPARC expression has not been examined in these.

SPARC has various biological functions relevant to soft tissue remodeling, including modulation of cell migration, proliferation and angiogenesis [21, 49, 73, 86, 209]. It has also been shown to affect morphology in a number of cell systems, particularly normal mesenchymal cells. It causes rounding of bovine aortic endothelial cells (BAE), fibroblasts and smooth muscle cells [49]. SPARC-null mesangial cells exhibit a flat morphology and an altered actin cytoskeleton, with vinculin-containing focal adhesions distributed over their center. In contrast, SPARC-null fibroblasts did not display any overt differences in cell morphology, and responded to exogenous rSPARC by rounding up in a manner similar to wild-type fibroblasts [76]. U87MG glioblastoma cells transfected with SPARC displayed a flatter morphology with extended cytoplasm instead of being round as expected [84]. In this study, we did not see any morphological effects of the induced SPARC on the MDA-MB-231 cells, nor when we added exogenous SPARC. It has been noted that SPARC effects on cell morphology are less apparent, or absent, in transformed cells [6].

Many of the reported effects of SPARC on cancer cells can be associated with poor outcome. U87 glioblastoma cells transfected with SPARC using tetracycline-inducible gene expression (Tet-Off) showed altered adhesion and increased invasion *in vitro* [84]. In a melanoma cell line, suppression of SPARC expression using antisense RNA significantly decreased *in vitro* adhesive and invasive capacities, and completely abolished *in vivo* tumorigenicity [35]. Additionally, a positive role of SPARC in the process of angiogenesis has been indicated [85]. In contrast, our transfected clones showed no increased migration or invasion *in vitro* in a variety of assays. This could be due to their carcinomatous nature, as ovarian carcinoma cells were also shown to be suppressed rather than stimulated by SPARC [75]. Different response profiles may be due to different SPARC receptors between cell types. Although cell-surface proteins have been shown to bind specifically to SPARC, there is no reported or characterized receptor for SPARC [53]. SPARC has also been shown to induce chemotactic migration of the MDA-MB-231 [73] but we did not assess this type of migration here.

SPARC has been shown to variably effect cell proliferation. In some cell types, SPARC seems to have no effect on growth while in others it is anti-proliferative [35, 73, 75]. We found an anti-proliferative effect in all of the transfected clones tested. This effect was not large but was highly reproducible, and stronger effects may have been seen if DOX had been continually added. This inhibition is consistent with that seen in ovarian carcinoma cells [75], and perhaps also with the increase in SPARC with differentiation of various systems, and its loss from certain systems upon transformation [6]. We do not know whether this anti-proliferative effect is direct or indirect, since SPARC has been found to associate with certain growth factors. It can bind to vascular endothelial growth factor (VEGF) and inhibit

VEGF-stimulated proliferation of human microvascular endothelial cells [77], and can counteract the proliferative effect of basic Fibroblast Growth Factor on smooth muscle cells [54]. DNA staining and cell cycle analysis showed a decreased proportion of cells in S-phase in a DOX concentration-dependent manner. This suggests an effect of SPARC on cell cycle progression to S phase in breast cancer cells, as has been reported for endothelial cells [74]. The cultured monolayer wound healing assay also confirmed the anti-proliferative effect of SPARC in the transfected clones, since the effect was abrogated when proliferation was blocked with thymidine. Although chemically modified tetracyclines can inhibit MDA-MB-468 human breast cancer cell proliferation [210], we never saw this effect on our parental cells with up to 2 µg/ml DOX and conclude that the effects that we saw were due to SPARC, not DOX.

In conclusion, the effect of SPARC on breast cancer cells reported here appears quite different to that seen in melanoma and glioma cell lines. SPARC did not effect cell morphology, adhesive properties, migration or invasion, but rather inhibited proliferation. This suggests that SPARC is a beneficial host factor in breast cancer, unlike what has been reported in melanoma, meningioma and glioma where SPARC seems to induce an invasive phenotype. Indeed, the higher levels of SPARC associated with more advanced breast cancers may represent an increased host effort to combat the carcinoma. Along these lines, an inverse correlation was seen between SPARC mRNA expression and estrogen receptor levels in breast tumour biopsies [83]. The results reported here indicate that further analysis of the biological consequences of SPARC in breast cancers is warranted.